ACS APPLIED POLYMER MATERIALS

pubs.acs.org/acsapm Article

Promising Chalcogenide Hybrid Copolymers for Sustainable Applications as Bio-lubricants and Metal Adsorbents

Juan Cubero-Cardoso, Antonio A. Cuadri, Fernando G. Fermoso, Jose Enrique Martín-Alfonso,* and Juan Urbano*

Cite This: *ACS Appl. Polym. Mater.* 2022, 4, 3667−3675

Read Online

ACCESS | Metrics & More | Article Recommendations

ABSTRACT: Inverse vulcanization has emerged as a reaction to achieve hybrid inorganic−organic polymeric materials, which allows us to use the high amount of sulfur produced during refining crude oil as a raw material. In this study, a gamut of copolymers has been formulated using a quantitative atom economy, that is, elemental sulfur and castor oil (CO), as can be seen from the appearance of gels to crystalline copolymers. The physical and chemical characterization has been carried out using techniques such as Fourier transform infrared spectroscopy, NMR, differential scanning calorimetry, and thermogravimetric analysis. Furthermore, two types of copolymers have been selected to test their capabilities in different applications. Copolymers with S ratios higher than 30% have been tested for water remediation, with high removal rates for metals such as lead and cadmium. Although copolymers with a percentage of up to 10% sulfur have been tested as bio-based lubricants, showing improvements in terms of viscosities compared to the initial vegetable oil.

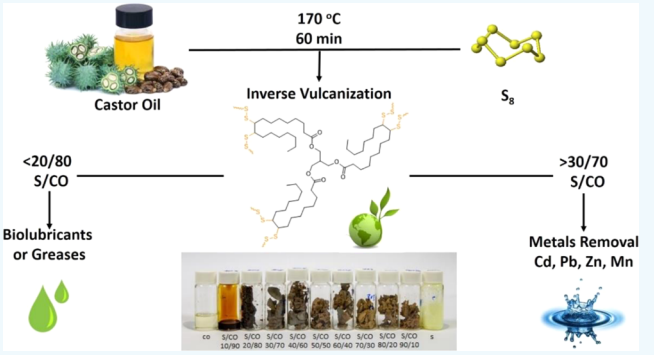

KEYWORDS: *green chemistry, agro-waste, petrochemical byproducts, inverse vulcanization, water remediation, bio-oil*

1. INTRODUCTION

In recent years, the need to establish sustainable processes has made the valorization of industrial byproducts a clear objective. In this context, an earth-abundant element that has been mined for thousands of years is elemental sulfur.[1] Sulfur is the 10th most abundant element on earth, and it is valuable for the scientific community as a chemical reagent with essential uses in industries, agriculture, or material science.[2,3] Until the 20th century, the most common source of sulfur was the soil surrounding volcanoes, but nowadays, starting with the development of the oil refining industry, the production of elemental sulfur (S_8) is achieved by removing the H_2S gas from crude oil. Around 50 million tons of sulfur are yearly obtained as a byproduct from the refining gas and petroleum industry.[4] Although there are different applications for the obtained sulfur, there is still a net excess of sulfur that offers little economic use.[5] Finding a large-scale use for this residual sulfur is nowadays a challenge for the environmentally friendly management and refining gas and petroleum industry.[6]

Recently, a polymeric reaction was developed by Pyun et al.,[7] called inverse vulcanization, which allows obtaining polymeric materials by the ring-opening polymerization (ROP) of elemental sulfur with other compounds bearing double bonds to form a class of hybrid inorganic−organic polymers (Figure 1). This process involves the melting of elemental sulfur at a temperature higher than 159 °C, during which the S_8 ring opens and polymerization can occur with other unsaturated cross-linkers. Polymers formed by inverse vulcanization have been found to have interesting optical, electrochemical, and self-healing properties.[8]

Most polymers are petroleum-based, and due to their high environmental impact, the synthesis of polymers from renewable sources is highly demanded by society and industries.[9] Carbon−carbon double bonds present in the triglycerides of vegetable oils are versatile cross-linkers for the inverse vulcanization process.[10] Unsaturated oils from olive, rapeseed, sunflower, and linseed plants are enticing options as cross-linkers. In general, vegetable oils are composed of some fatty acids that, depending on the plant source, have different numbers of double bonds.[10] Castor oil (CO) is an exciting option as raw material for inverse vulcanization as its toxicity does not allow it to be used for human consumption.[11]

Received: February 2, 2022
Accepted: April 19, 2022
Published: May 3, 2022

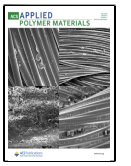

https://doi.org/10.1021/acsapm.2c00209
ACS Appl. Polym. Mater. 2022, 4, 3667−3675

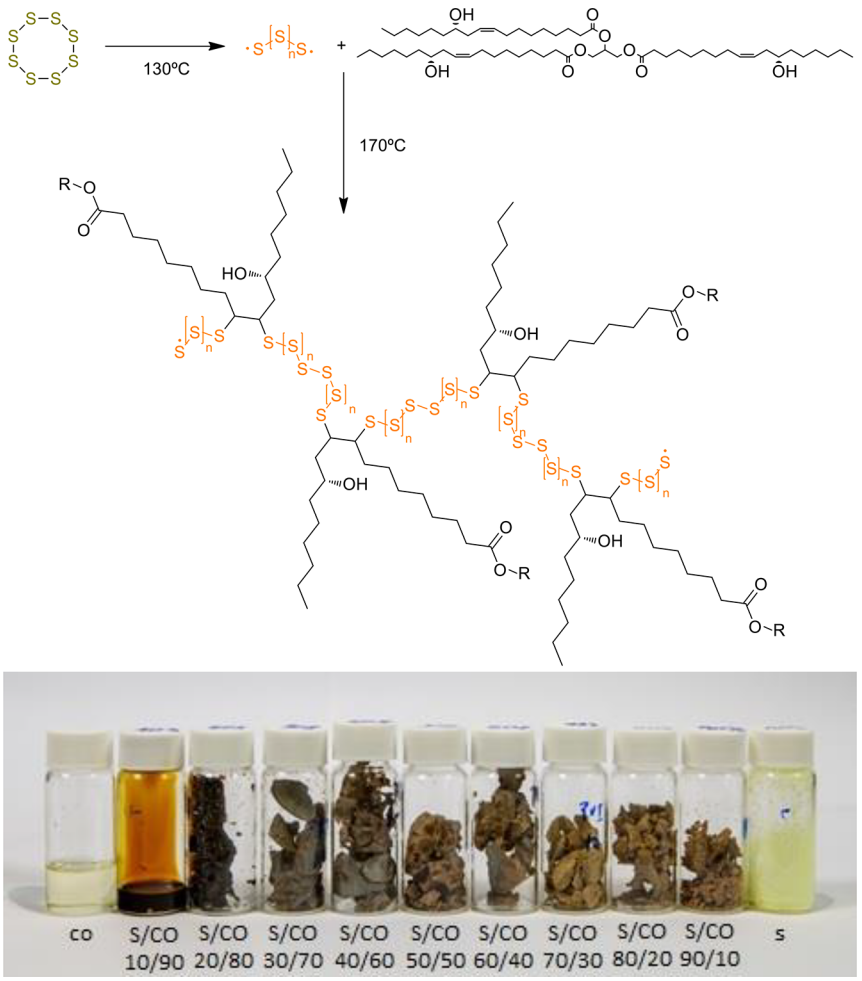

Figure 1. Inverse vulcanization reaction with CO and images of different copolymers obtained with different ratio (S/CO) w/w %.

The properties of the polymers produced by the inverse vulcanization process are controlled by selecting the polymerization reaction conditions and using different vegetable oils, obtaining a wide variety of properties.[12,13] These properties can range from highly cross-linked thermosets to linear thermoplastics.[14] For example, sulfur copolymers obtained by inverse vulcanization of elemental sulfur and vegetable oils such as sunflower, olive, and linseed have been applied in the development of lithium−sulfur battery cathodes proved a remarkable preliminary specific capacity as a battery.[15] In another study, soybean oil was chosen to react with elemental sulfur to obtain a solid fertilizer for plants as a sulfur source.[16−18] Even canola oil and recycled cooking oils have been used to produce a sulfur-based polymer that exhibited a significant effect as an adsorbent for mercury contamination.[8,19,20] Indeed, due to the high soft−soft Lewis acid interaction, the sulfur content of these polymers causes an affinity for heavy metals.[10,21] The European Directive Commission Decision 05/360/EC[22] has given exceptional attention to the protection against pollution caused by lubricants and hydraulic fluids based on mineral oils. Hybrid inorganic−organic polymers produced from inverse vulcanization and based on vegetable oils as bio-based lubricating fluids might replace such lubricants and hydraulic fluids based on mineral oils. However, there are no significant numbers of studies about producing such hybrid inorganic−organic polymers as a lubricant or hydraulic fluid.[23,24]

The aim of this work is to synthesize and characterize a hybrid inorganic−organic polymer produced by inverse vulcanization using residual sulfur coming from the refining petroleum industry and CO as vegetable oil. The produced polymer will be assessed as adsorbents for heavy metal remediation and as a lubricant.

2. EXPERIMENTAL SECTION

2.1. Raw Materials. CO was supplied by Guinama (Valencia, Spain), and elemental sulfur 99% was supplied by the refining petroleum company CEPSA (Huelva, Spain). Both reagents were used as received. CO fatty acid composition is shown in Table 1 as reported by the supplier.

2.2. Preparation of Poly(S/CO) Formulations. Inverse vulcanization of elemental sulfur and CO was carried out following a slight modification of Chalker's preparation.[10] Elemental sulfur (S_8) was heated and melted under vigorous stirring at 130 °C. At this point, CO was slowly added continuously up to 170 °C, where ROP was achieved at the desired w/w ratio (Figure 2). Blends were stirred for 60 min maintaining the temperature to finish the comonomer conversion. Copolymers appeared from viscous oleogels to solid brown rubbers. More brittle copolymers are obtained as the S content increases.

2.3. Adsorption Experiments. Four metals were selected for this study, that is, cadmium (Cd), lead (Pb), zinc (Zn), and manganese (Mn). Cadmium(II) [$Cd(NO_3)_2{\cdot}4H_2O$], lead(II) [$Pb(NO_3)_2$], zinc(II) [$Zn(NO_3)_2{\cdot}6H_2O$], and Mn(II) [$Mn(SO_4){\cdot}H_2O$] were chosen as the salts for the corresponding metal source. A solution for each metal was made at 100 mg salt per liter. Batch adsorption

https://doi.org/10.1021/acsapm.2c00209
ACS Appl. Polym. Mater. 2022, 4, 3667−3675

Table 1. Fatty Acid Nature and Concentration for CO

fatty acids (%)	castor oil
myristic C14:0	trace
palmitoleic C16:0	1.70
palmitoleic C16:1	trace
stearic C18:0	1.96
oleic C18:1	5.34
ricinoleic C18:1:OH	82.48
linoleic C18:2	7.01
linolenic C18:3	1.51
arachidic C20:0	trace
lignoceric C24:0	trace
saturated	3.66
monounsaturated	87.82
polyunsaturated	8.52

experiments for each metal with 30, 70, 80, and 100% S/CO copolymers were performed thrice during two different adsorption times, 1 and 24 h. 20 mL of the aqueous solution was added together with 1 g of the S/CO copolymer into a 50 mL vial equipped with a magnetic stirring bar and stirred for 1 or 24 h of adsorption time.

2.4. Structural Analysis of Sulfur Copolymers. Fourier transforms infrared (FTIR) spectra were registered in the absorbance mode within a wavenumber range of 400−4000 cm^{-1} at 4 cm^{-1} resolutions using an FT/IR-4200 apparatus (Jasco Analytical Instrument, Japan). In the transmission mode, were performed a total of 46 scans for each sample. In addition, an attenuated total single reflection accessory fitted with a diamond crystal has been used for surface FTIR analyses of the films.

Thermal characterization of S/CO copolymers was performed using a differential scanning calorimeter to provide information about the homogeneity of the polymers by detecting any thermal events. Differential scanning calorimetry (DSC) measurements were performed with a TA Q-100 (TA Instruments, USA). At least two replicates of 4−6 mg samples sealed in hermetic aluminum pans were purged with nitrogen at a 50 mL/min flow rate. Calibration of temperatures and enthalpy was performed with standard indium, using thermal software version 4.0. Heat flow curves were obtained by applying a temperature program of 0 to 180 °C/180 °C to 0 °C/0 to 180 °C, at 10 °C/min. The significant events were determined from the second scan to cancel the effect of aging on the morphology of the samples [glass transition (T_g), cold crystallization (T_{cc}), melting temperatures (T_m), cold crystallization (ΔH_{cc}), and melting enthalpies (ΔH_m)].

The thermal resistance of S/CO copolymers was studied using thermogravimetric analysis (TGA), which provides information on the thermal decomposition of these systems. TGA was carried out under a N_2 purge using TA Q-50 (TA Instruments, USA). Approximately 8−10 mg of each sample was placed on a Pt pan under N_2 gas flow at 100 mL/min and heated from 30 to 500 °C at 10 °C/min.

The prepared poly(S/CO) copolymers were also characterized by solution NMR. ^{1}H NMR spectroscopy was used to determine the chemical structures of the poly(S/CO) copolymers. Nuclear magnetic resonance spectroscopy (^{1}H NMR) of CO and 10, 30, and 80% of (S−CO) copolymer samples was recorded at 500 MHz using a Varian Mercury 500 spectrometer. Deuterated pyridine-d_5 was used as a solvent. ^{1}H NMR shifts are reported relative to tetramethylsilane.

The concentration of all metals was measured using an atomic absorption spectrometer SpectrAA 50B (Varian). Calibration standard solutions were run prior to each analysis. Spectrograms of both standard and sample solutions of Cd, Pb, Zn, and Mn have been recorded by measuring the absorbance at 222.6, 228.8, 283.3, and 403.1 nm, respectively.

Dynamic viscosities were measured for two replicates in a rotational controlled strain rheometer, model ARES (Rheometric Scientific, UK), in a temperature range between 25 and 120 °C.

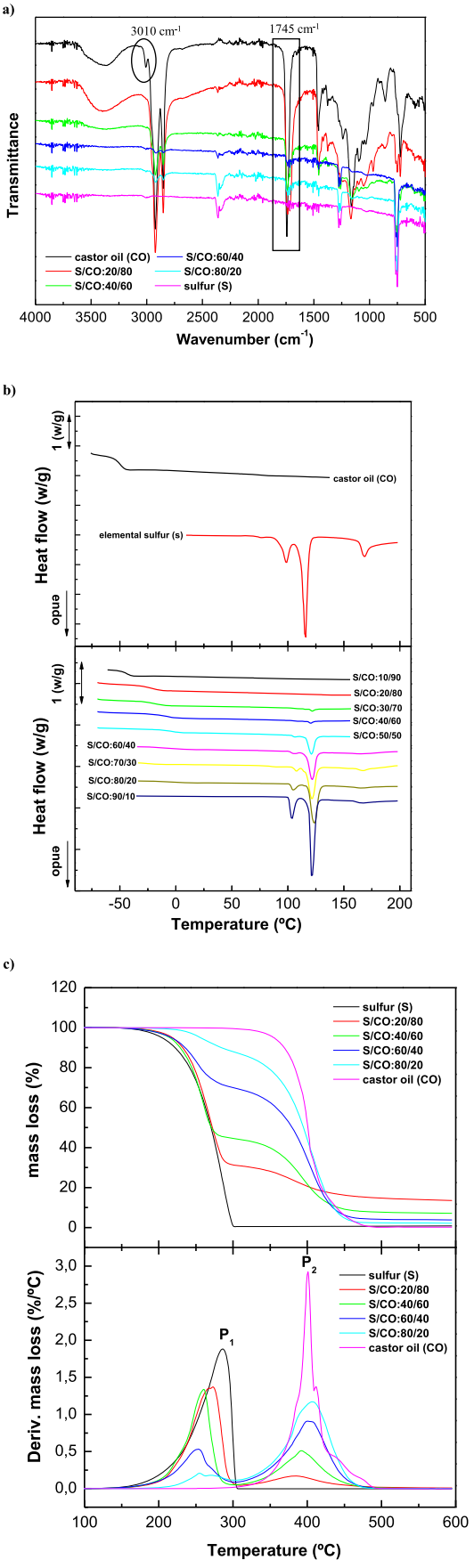

Figure 2. (a) FTIR spectra, (b) DSC heat flow curves, and (c) TGA thermograms of CO, elemental sulfur, and (S/CO) copolymers as a function of the ratio of S/CO.

https://doi.org/10.1021/acsapm.2c00209
ACS Appl. Polym. Mater. 2022, 4, 3667−3675

Viscous flow test was carried out in a shear rate range of 5−5000 s^{-1}, using a Couette geometry (inner radius: 16 mm, outer radius: 17 mm, and cylinder length: 33.5 mm).

3. RESULTS AND DISCUSSION

3.1. FTIR Measurements from CO and Copolymers. FTIR spectra of elemental sulfur, CO, and selected S/CO copolymers are shown in Figure 2a. The hydroxyl group of CO appears in the peaks at 3380 cm^{-1} and 3010 cm^{-1}, confirming the presence of C═C from ricinoleic acid. Other intense peaks appeared at 2926 and 2852 cm^{-1}, which arose from C−H asymmetric stretch vibration in CH_3 and CH_2. The peak at 1745 cm^{-1} was ascribed to a carbonyl group (C═O).[25] FTIR spectra of S/CO copolymers are very close to those of CO. The signals at 3010 and 1745 cm^{-1} represented vinylic C−H bonds and C═C double bonds, respectively. As can be observed in Figure 2a, these peaks disappeared for S/CO copolymers, indicating that the addition of sulfur to the double bonds is quantitative, which revealed the participation of sulfur in the copolymer formation. After the reaction, the characteristic peaks at 803 and 967 cm^{-1} appeared for S/CO polymers. These are attributed to C−H rocking vibrations in the vicinity of a C−S bond. In addition, around 700 cm^{-1}, a peak with reduced intensity could be attributed to the C−H out-of-plane deformation vibration of a double bond and is another indicator of the favorable C−S chemical reaction. Similar results were found by Hoefling et al.[15] for linseed oil−sulfur-based materials.

3.2. DSC Properties from CO and Copolymers. Thermal characterization of S/CO copolymers was performed using differential scanning calorimeter to provide information about the homogeneity of the polymers by detecting any thermal events. Figure 2b shows the DSC thermograms of CO and sulfur used as raw materials to prepare S/CO copolymer formulations. It can be seen that the CO heat flux curve shows an endothermic peak, which is related to the crystallization event that occurs at low temperatures. Depending on the diversity in the composition of the fatty acids, the crystallization of the oil will occur in a wide range of temperatures.[26] The elemental sulfur used shows two melting peaks (at 98 and 115 °C) attributed to the fusion of the monoclinic and the orthorhombic sulfur, respectively. On the other hand, Figure 2b displays the heat flow curves for S/CO copolymers. As can be seen, all samples present one thermal event at low temperatures, more apparent when CO content increases, corresponding to the glass transition temperatures (T_g) of the copolymers, ranging from −40 to −2 °C depending on the S/CO ratio (Table 2). The glass transition temperature increases with increasing sulfur content, suggesting a decrease in flexibility of samples due to a highly cross-linked network. Interestingly, on increasing sulfur content above 20 wt %, there was an endothermic event between 95 and 135 °C. This transition was attributed to the melting range of unreacted sulfur. By integrating areas of each of these endothermic peaks, an estimate of unreacted sulfur was made (Table 2). For instance, the S/CO: 50/50 sample was estimated to contain about 9 wt % free sulfur. These results have shown the idea that sulfur reacted with CO to form a cross-linked polymer up to a composition of about 20% sulfur. In a copolymer above this percentage, the excess sulfur remains dispersed in the polymer matrix in the form of granules or microparticles, modifying the microstructure.

Table 2. Characteristic Parameters Obtained from DSC Measurements of the (S/CO) Copolymers

samples	T_g (°C)	(ΔH_m) (J/g)	free S_8 (wt %)
sulfur (S)		31.9	
S/CO: 10/90	−43.2		
S/CO: 20/80	−21.9		
S/CO: 30/70	−16.8	2.0	3
S/CO: 40/60	−11.2	3.1	4
S/CO: 50/50	−4.4	14.2	9
S/CO: 60/40	−0.75	22.8	21
S/CO: 70/30	−24.5	28.7	23
S/CO: 80/20	−2.30	34.2	29
S/CO: 90/10		55.3	56
castor oil (CO)	−51.6		

3.3. TGA Properties from CO and Copolymers. The thermal resistance of (S/CO) copolymers has been studied employing TGA, which offers information on the thermal decomposition of the copolymers. Figure 2c shows the variation of the experimental mass loss (TG) and mass loss rate (DTG) with temperature for elemental sulfur, CO, and (S/CO) copolymers as a function of the ratio of S/CO. As may be observed, thermal decomposition of the elemental sulfur and CO takes place in one single degradation stage, attributable to the loss of sulfur and volatile sulfides in the first case and the second being mainly related to the decomposition and/or volatilization of fatty acids, the most concentrated one, that is, the ricinoleic fatty acid, and subsequent degradation compounds. By contrast, thermal decomposition of (S/CO) copolymers occurs in just two stages, identical for all the samples studied. The first stage, happening in the temperature range 205−358 °C, is attributable to the departure of the decomposition of polysulfide domains from the sample. The second stage, occurring between 298 and 502 °C, corresponds to the thermal decomposition of the CO domain of the polymer. The magnitude of these degradation stages is dependent on the composition of (S/CO) copolymers. Thus, the first decomposition gradually increases as sulfur content increases. Table 3 shows characteristic parameters of these curves, that is, the temperature for the onset of thermal decomposition (T_{onset}), the temperature at which the decomposition rate is maximum (T_{max}), and the percentage of non-degraded residue for elemental sulfur, CO, and (S/CO) copolymers. Based on these data, the T_{onset} and the T_{max} (only P_2) took place at lower values when the CO content of the (S/CO) copolymer was increased. Interestingly, it is worth noting that the residue of the polymers with the lowest amount of sulfur (10 and 20%) shows higher values than other polymers. This behavior can be explained considering that sulfur and CO reacted up to a composition of 20% sulfur, which was also corroborated by DSC results.

3.4. Structural Analysis via Solution NMR Spectroscopy. The prepared (S/CO) copolymers were also monitored by solution NMR. ^{1}H NMR spectroscopy was used to determine the chemical structures of the four series of (S/CO) copolymers. The representative ^{1}H NMR spectra of copolymers with 10, 30, 50, and 80% sulfur content are displayed in Figure 3. Due to the low solubility of the synthesized copolymers in most common organic solvents, except in pyridine in which the copolymers were broken down and dissolved entirely,[10,27] the reaction monitoring was carried out in deuterated pyridine to obtain good-quality solution

https://doi.org/10.1021/acsapm.2c00209
ACS Appl. Polym. Mater. 2022, 4, 3667−3675

Table 3. Characteristic Parameters Obtained from TGA Measurements of the Poly(S/CO) Copolymers

samples	T_{onset} (°C)	decomposition temperature range (°C)	T_{max} (°C)		residue^{600} (%)
			P_1	P_2	
sulfur (S)	204.5	204.5−307.6	285.8	0	0.43
S/CO: 10/90	218.1	218.1−358.3/358.3−493.6	275.4	399.9	14.8
S/CO: 20/80	218.2	218.2−307.7/307.7−500.1	273.1	385.1	14.2
S/CO: 30/70	205.8	205.8−300.7/300.7−502.4	258.5	389.9	6.35
S/CO: 40/60	215.1	215.1−300.8/300.8−501.7	260.6	392.3	7.60
S/CO: 50/50	210.3	210.3−300.4/300.4−502.7	261.6	392.2	8.55
S/CO: 60/40	217.5	217.5−300.5/300.5−498.1	253.7	400.1	4.19
S/CO: 70/30	227.1	227.1−304.1/304.1−493.5	252.4	405.5	2.67
S/CO: 80/20	256.6	256.6−304.1/304.1−487.3	255.1	406.8	2.41
S/CO: 90/10	312.8	312.8−297.1/297.5−492.1	266.3	411.7	0.72
castor oil (CO)	355.3	355.3−489.1	0	400.7	0.17

NMR data, as has been seen in similar studies.[10,27] As can be observed in Figure 3b, the alkene $=CH_2$ proton peaks at δ = 5.1 and δ = 5.4 ppm are completely absent for samples with a S/CO ratio comprising above 30% sulfur. This indicates that for these samples, the vegetable oil has reacted completely with sulfur. Conversely, for copolymers with sulfur content below 30%, there are still signals attributed to unreacted alkene groups in the final product. It is reasonable that these copolymers with a low amount of sulfur lead to an incomplete cross-linking reaction. To verify this assumption, an NMR diffusion experiment was developed to characterize the lightest fraction of the (S/CO) copolymer with a phase-edited DOSY. In Figure 3c, a DOSY spectrum of the (S/CO: 10/90) mass percentage copolymer is presented. In the case of a mixture of several compounds, either the starting material or different copolymers, different groups of signals should be seen; however, in this case, only a single group of signals is observed, thus indicating that a single type of copolymer has been formed. Regarding the new C−S bonds that should appear in the ^{1}H spectra, previous studies showed that these copolymers based on sulfur should present signals due to the thiol group between 1 and 3.5 ppm.[28] They are attributed to the high activity of sulfide radicals toward hydrogen abstraction during the inverse vulcanization process. However, these signals are not observed in Figure 3b because they probably overlap with those of CO comonomers. To support this assumption, FTIR spectroscopy can be used; in Figure 2a, the FTIR spectra of different copolymers show a weak signal at 2400 cm^{-1} that increases in intensity when the amount of sulfur in the copolymer increases. This new signal is not displayed in the spectra for the raw CO, and therefore it can be attributed to the new −SH− groups. In the same way, when −SH groups are formed, hydrogen sulfide (H_2S) should be released. To verify this assumption, all the gases formed were bubbled through a solution of 1 M of silver nitrate ($AgNO_3$) during the inverse vulcanization reaction. Immediately, the clear solution turned dark brown, and a black solid (Ag_2S) was settled.

3.5. Metal Adsorption Capacity of the (S/CO) Copolymer. The poly(S/CO) has been used to comply with the European directive[22] on water policies. Some metals are classified as priority pollutants, that is, Hg, Cd, Pb, Zn, Ni, Cu, Cr, As, and Se. For this reason, the environmental remediation-mediated heavy metal adsorption would be a greener utilization strategy. The influence of the (S/CO) copolymer ratio and contact time on metal adsorption has been shown in Figure 4a. At 1 h contact time, only 25 and 50% of the four metals have been removed under the study, showing no significant difference in the removal of these metals between the polymers and elemental sulfur. Furthermore, based on Pearson theory, the interactions between soft acid and soft base have been observed, leading to a percentage around 50%, affirming the affinity of heavy metals, such as lead and cadmium, toward sulfur.[29] However, in the case of harder elements such as manganese and zinc, this interaction is not as satisfactory and remains almost constant in all the attempts. Different studies have shown Lewis−Lewis soft interaction with metals cations, that is, mercury adsorption is effective with sulfur and vegetable oil copolymers because it is a soft metal.[8,10,30] To avoid this behavior, the synthesis of next generation of the hybrid copolymer to improve this affinity to hard metals is currently under investigation in our laboratory.

To improve the removal capacity, the contact time for each experiment was increased until 24 h. The removal percentage of lead and cadmium increases when the S/CO ratio increases, reaching the highest retention capacity for lead and cadmium at 80% S. It is worth noticing that zinc retention capacity at 1 and 24 h was similar. Therefore, the retention capacity of zinc was only influenced by the S content of the copolymer. This study confirmed the efficient adsorption of different metals when sulfur/refined oil ratios and time increase. Under the conditions of assays, the percentage of removal of all metals has increased concerning others studies,[29,30] that is, less than 20% removal and focusing on mercury (Table 4).

Based on the polymer material with the best adsorbent capacity (poly S/CO: 80/20), a series of experiments were carried out to obtain the best dosage ratio. It has been proposed to study the adsorbent dosages, modifying the volume of the solution of the metals (500, 100, 40, 20, and 10 mL) and maintaining the concentration of each metal and weight of the adsorbent material [100 mg L^{-1} and 1 g of (S/CO: 80/20) copolymer]. For cadmium, a linear trend can be observed that goes from 15 to 100% removal (Figure 4b). For lead and zinc, the same trend for Cd has been observed, reaching removal from 19 to 88% for Pb and 62% for Zn. The capacity to remove manganese reached less than 20%, showing that this copolymer is not selective for Mn, as shown in the assay at different contact times.

3.6. Lubricant Behavior of the (S/CO) Copolymer. Due to the versatility of the S/CO copolymers in terms of their physical behavior, the lightest fraction has appeared as oleogel, that is, 10% of sulfur content, and it could be considered a viable bio-lubricant. The DOSY spectra confirmed the (S/CO: 10/90) copolymer to be a simple reticulated copolymer, not a

https://doi.org/10.1021/acsapm.2c00209
ACS Appl. Polym. Mater. 2022, 4, 3667−3675

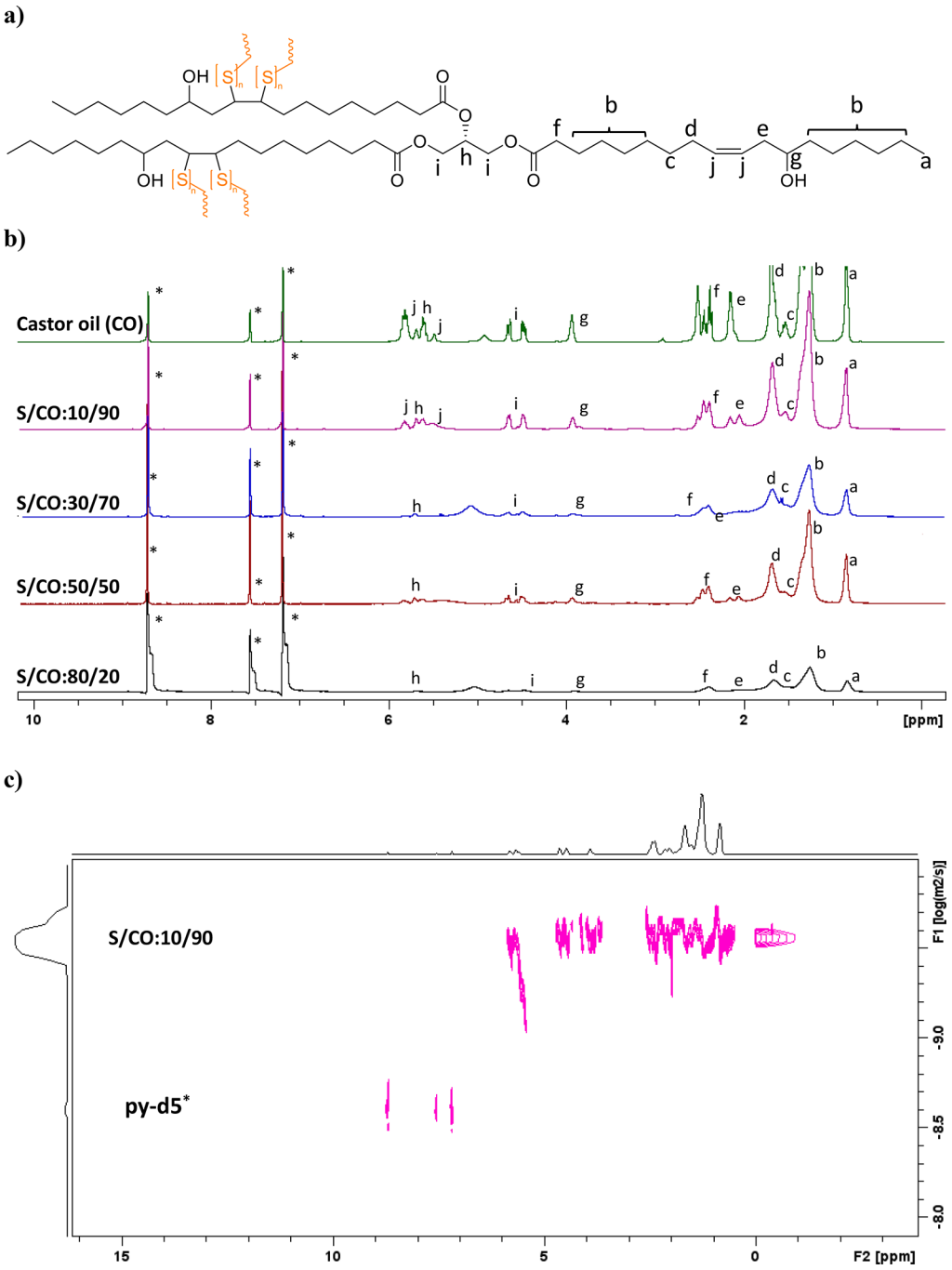

Figure 3. (a) Representative structure of the (S/CO) copolymer, (b) ^{1}H NMR spectra of (S/CO) copolymers as a function of the ratio of S/CO, and (c) DOSY spectra for the (S/CO: 10/90) copolymer.

mixture (Figure 3c). Figure 5a shows the viscosity at 23 °C of CO and (S/CO: 10/90) copolymers with increasing shear stress, and it was observed that the model copolymer behaves like a Newtonian fluid and shows that it has almost ten times more viscosity compared to the CO.

The small-amplitude oscillatory shear results are presented in Figure 5b. It was observed that in both cases, the viscous or loss modulus (G'') predominates over the elastic or storage modulus (G'), that is, $G'' > G'$. As can be seen in Figure 5b, the 10% S/CO copolymer exhibits significantly higher G' and G'' values than the original CO. Furthermore, for the two compounds, G'' increased more than a decade compared to G' in the frequency range studied. This denotes the predominant character of the CO and (S/CO: 10/90) copolymer as a liquid than as a viscoelastic fluid. In a general manner, this trend is reversed on increasing frequency, and when G' is greater than G'', the material will behave as a solid, not a liquid.[26,32]

Regarding viscous flow characterization, in Table 5, dynamic viscosities for the original CO and the (S/CO: 10/90) copolymer within a temperature range of 25 up to 100 °C are presented. In the case of the (S/CO: 10/90) copolymer, it shows much higher viscosities than CO, probably attributed to the interaction forces among CO−sulfur oleogel. Unfortunately, this kind of interaction forces is more dependent on temperature, and the final valor decreases at 100 °C in both cases. In order to obtain thermodynamics data, the Arrhenius-

https://doi.org/10.1021/acsapm.2c00209
ACS Appl. Polym. Mater. 2022, 4, 3667−3675

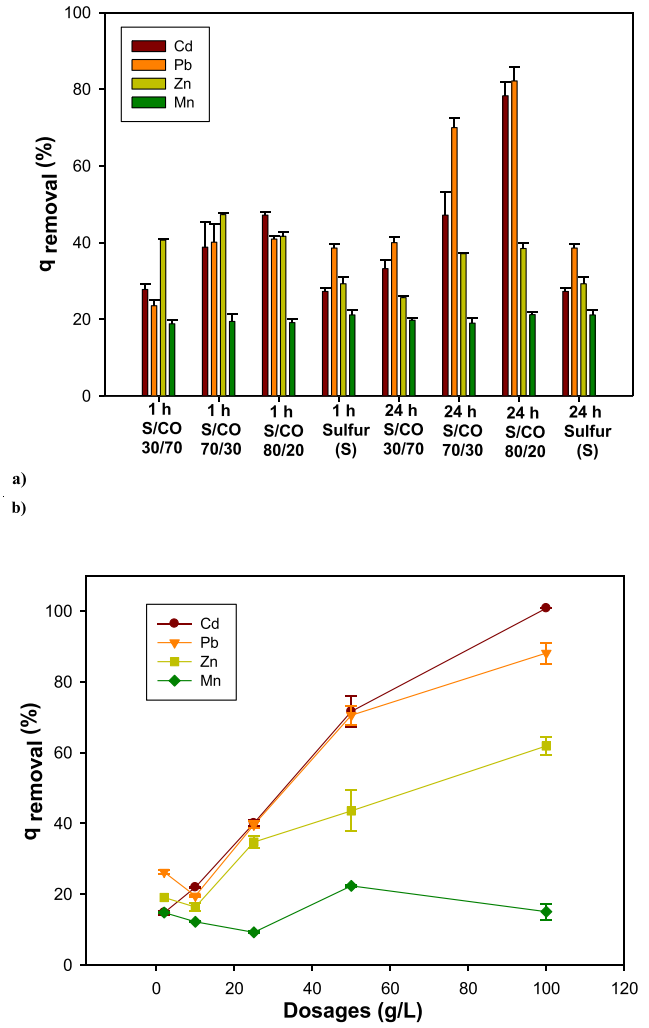

Figure 4. (a) Effect of the adsorption time and S/CO ratio on the metal adsorption over copolymers at 30, 70, and 80% sulfur (S) during 1 and 24 h. Conditions: adsorption dosage, 50 g L^{-1}; concentration of each ion: 100 mg L^{-1}; and T^a: 25 °C. (b) Effect of an adsorbent dosage on Cd, Pb, Zn, and Mn removal with the (S/CO: 80/20) copolymer.

type equation has been implemented (eq 1) to fit the evolution of viscosity of both compounds with the temperature[33]

$$\eta = A\, e^{E_a/RT} \quad (1)$$

where η is the dynamic viscosity, A is the pre-exponential factor, E_a is the activation energy, R is the gas constant (8.314 J mol^{-1} K^{-1}), and T is the temperature (K). As can be observed in Table 5 (S/CO: 10/90), the copolymer presents higher activation energy than CO, that is, 60.7 kJ/mol. To test if the measured (S/CO: 10/90) copolymer could be a suitable

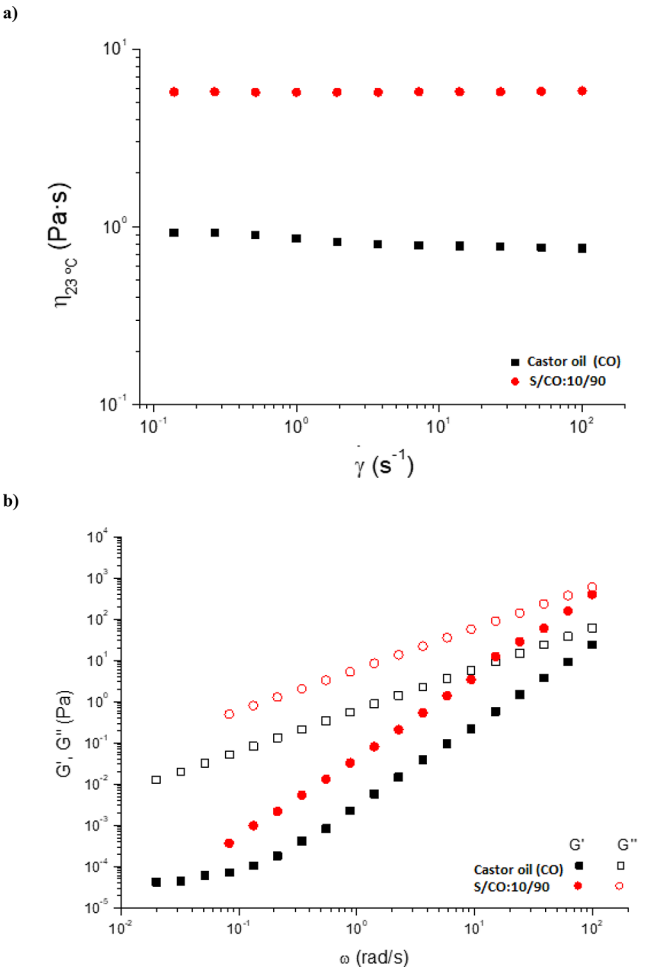

Figure 5. (a) Viscosity of CO and (S/CO: 10/90) copolymers and (b) frequency modulus dependence of the storage, G', and loss, G''.

Table 5. Dynamic Viscosity and Fit Parameters of the Arrhenius Equation for the (S/CO) Copolymer S/CO: 10/90 Compared to Castor Oil Obtained in the Study by Quinchia et al.[41]

	S/CO: 90/10	castor oil	$\Delta\mu$ (S/CO)
T °C	μ (Pa s)	μ (Pa s)	μ (Pa s)
25	51.4	5.5×10^{-1}	51.341
40	14.1	2.3×10^{-1}	14.071
60	2.99	7.6×10^{-2}	2.972
70	1.67	4.9×10^{-2}	1.656
80	0.932	3.4×10^{-2}	0.921
100	0.338	1.9×10^{-2}	0.331
A (Pa s)	60.7×10^{-10}	4.5×10^{-8}	-3.893×10^{-8}
E_a (kJ/mol)	60.7	40.1	20.6

Table 4. Different Studies Based on (S-Vegetable Oil) Copolymers on the Removal of Heavy Metals

oils	S_8 (%)	T °C	time (min)	dosage (g L^{-1})	ion concentration (mg L^{-1})	time (hour)	removal (%)	references
canola	50 + NaCl	175	12	50	$HgCl_2$ 107	24	92	10
rice bran	50 + NaCl	175	25	50	$HgCl_2$ 107	24	82	10
castor	50 + NaCl	175	21	50	$HgCl_2$ 107	24	83	10
canola	50	180	20	400	$HgCl_2$ 20	24	54	8
cottonseed	50	150	30	3 (pH 6)	$HgCl_2$ 358.5	10	over 80	31
canola	50 + NaCl	170	25	80	$Pb(NO_3)_2$ 560	1	2.8	20

https://doi.org/10.1021/acsapm.2c00209
ACS Appl. Polym. Mater. 2022, 4, 3667−3675

hydraulic fluid, it would be necessary to measure the kinematic viscosity. Still, these preliminary experiments only intended to show that a more viscous fluid than vegetable oil has been formulated. CO−sulfur oleogel could be an interesting option for use as cutting fluids because it presents a proven antioxidant and antimicrobial capacity[34−36] and good thermal stability.[37] Possible use of these liquid copolymers could be their use as cutting fluids[38,39] because the presence of sulfur in their structure could have enhanced properties.[23,24,37] In contrast, the stability of vegetable oils as lubricating agents under severe operating conditions is low.[40]

4. CONCLUSIONS

We report the synthesis and characterization of a gamut of hybrid inorganic−organic copolymers based on vegetable oil and elemental sulfur through inverse vulcanization. The CO was used as an effective organic cross-linker inspired by organic polymerization processes. Ratios from 10 to 90% sulfur gave rise to a gamut of copolymers with different physical properties from oleogels to crystalline copolymers. Based on their physical properties, the higher amount of sulfur fractions was chosen to remove metals in water the (S/CO: 80/20) copolymer. Almost quantitatively, the softer metallic elements, that is, lead and cadmium, were removed, compared with the harder ones, such as zinc and manganese, which had a low withdrawal result. In the case of oleogels to 10% sulfur (S/CO: 10/90) copolymers, this copolymer was tested as a precursor of bio-based lubricants. The copolymer presented almost 10 times more viscosity and higher activation energy, that is, 60.7 kJ/mol, concerning the CO.

AUTHOR INFORMATION

Corresponding Authors

Jose Enrique Martín-Alfonso − *Department of Chemical Engineering and Materials Science, Chemical Product and Process Technology Research Center (Pro2TecS), University of Huelva, 21071 Huelva, Spain*; Email: jose.martin@diq.uhu.es

Juan Urbano − *Laboratory of Sustainable and Circular Technology, CIDERTA and Chemistry Department, Faculty of Experimental Sciences, University of Huelva, 21071 Huelva, Spain*; orcid.org/0000-0001-7368-9492; Email: juan.urbano@dqcm.uhu.es

Authors

Juan Cubero-Cardoso − *Laboratory of Sustainable and Circular Technology, CIDERTA and Chemistry Department, Faculty of Experimental Sciences, University of Huelva, 21071 Huelva, Spain; Instituto de Grasa, Spanish National Research Council (CSIC), 41013 Seville, Spain*; orcid.org/0000-0002-4455-5417

Antonio A. Cuadri − *Department of Chemical Engineering and Materials Science, Chemical Product and Process Technology Research Center (Pro2TecS), University of Huelva, 21071 Huelva, Spain*; orcid.org/0000-0002-8289-0937

Fernando G. Fermoso − *Instituto de Grasa, Spanish National Research Council (CSIC), 41013 Seville, Spain*; orcid.org/0000-0002-2586-007X

Complete contact information is available at: https://pubs.acs.org/10.1021/acsapm.2c00209

Author Contributions

Conceptualization, J.C.-C., A.A.C., J.E.M.-A., and J.U.; methodology, J.C.-C., A.A.C., J.E.M.-A., and J.U.; resources, F.G.F. and J.U.; writing—original draft preparation, J.C.-C. and A.A.C.; writing—review and editing, J.E.M.-A., F.G.F., and J.U.; supervision, J.U.; funding acquisition, F.G.F, and J.U. All authors have read and agreed to the published version of the article.

Funding

The authors thank financial support from Junta de Andalucía, Consejería de Economía y Conocimiento, and University of Huelva (P.O. Feder UHU-1257728).

Notes

The authors declare no competing financial interest.

ACKNOWLEDGMENTS

The authors want to express their acknowledgement for Fundación Cátedra Cepsa for kindly supplying the sulfur and the Center for Research in Sustainable Chemistry—CIQSO for NMR facilities. We thank Francisco Molina for support with NMR studies. We also wish to thank the referees for their valuable contributions. Funding for open access charges is given by Universidad de Huelva/CBUA.

REFERENCES

(1) Nguyen, D.-T.; Horia, R.; Eng, A. Y. S.; Song, S.-W.; Seh, Z. W. Material Design Strategies to Improve the Performance of Rechargeable Magnesium−Sulfur Batteries. *Mater. Horiz.* **2021**, *8*, 830−853.

(2) Boyd, D. A. Sulfur and Its Role In Modern Materials Science. *Angew. Chem., Int. Ed.* **2016**, *55*, 15486−15502.

(3) Lee, T.; Dirlam, P. T.; Njardarson, J. T.; Glass, R. S.; Pyun, J. Polymerizations with Elemental Sulfur: From Petroleum Refining to Polymeric Materials. *J. Am. Chem. Soc.* **2022**, *144*, 5−22.

(4) Zharylkassyn, P.; Ramatullaeva, L.; Shapalov, S.; Kenzhaliyeva, G.; Kocherov, Y.; Zhumadullayev, D. Formulation of Composite Materials Containing Tengiz Sulfur-Oil Production Waste. *Ecol. Eng. Environ. Technol.* **2021**, *22*, 66−73.

(5) Khan, S. H.; Amani, S.; Amani, M. Alternative and Potential Uses for the Sulfur Byproducts Produced from Oil and Gas Fields. *Int. J. Org. Chem.* **2021**, *11*, 14−23.

(6) Zhang, Y.; Glass, R. S.; Char, K.; Pyun, J. Recent Advances in the Polymerization of Elemental Sulphur, Inverse Vulcanization and Methods to Obtain Functional Chalcogenide Hybrid Inorganic/Organic Polymers (CHIPs). *Polym. Chem.* **2019**, *10*, 4078−4105.

(7) Chung, W. J.; Griebel, J. J.; Kim, E. T.; Yoon, H.; Simmonds, A. G.; Ji, H. J.; Dirlam, P. T.; Glass, R. S.; Wie, J. J.; Nguyen, N. A.; Guralnick, B. W.; Park, J.; Somogyi, Á.; Theato, P.; Mackay, M. E.; Sung, Y.-E.; Char, K.; Pyun, J. The Use of Elemental Sulfur as an Alternative Feedstock for Polymeric Materials. *Nat. Chem.* **2013**, *5*, 518−524.

(8) Worthington, M. J. H.; Kucera, R. L.; Albuquerque, I. S.; Gibson, C. T.; Sibley, A.; Slattery, A. D.; Campbell, J. A.; Alboaiji, S. F. K.; Muller, K. A.; Young, J.; Adamson, N.; Gascooke, J. R.; Jampaiah, D.; Sabri, Y. M.; Bhargava, S. K.; Ippolito, S. J.; Lewis, D. A.; Quinton, J. S.; Ellis, A. V.; Johs, A.; Bernardes, G. J. L.; Chalker, J. M. Laying Waste to Mercury: Inexpensive Sorbents Made from Sulfur and Recycled Cooking Oils. *Chem.—Eur. J.* **2017**, *23*, 16219−16230.

(9) Mendes, A. C.; Pedersen, G. A. Perspectives on Sustainable Food Packaging: Is Bio-Based Plastics a Solution? *Trends Food Sci. Technol.* **2021**, *112*, 839−846.

(10) Tikoalu, A. D.; Lundquist, N. A.; Chalker, J. M. Mercury Sorbents Made By Inverse Vulcanization of Sustainable Triglycerides: The Plant Oil Structure Influences the Rate of Mercury Removal from Water. *Adv. Sustainable Syst.* **2020**, *4*, 1900111.

(11) Park, K. W.; Leitao, E. M. The Link to Polysulfides and Their Applications. *Chem. Commun.* **2021**, *57*, 3190−3202.
(12) Chen, Y.; Liu, Y.; Chen, Y.; Zhang, Y.; Zan, X. Design and Preparation of Polysulfide Flexible Polymers Based on Cottonseed Oil and Its Derivatives. *Polymer* **2020**, *12*, 1858.
(13) Chalker, J. M.; Worthington, M. J. H.; Lundquist, N. A.; Esdaile, L. J. Synthesis and Applications of Polymers Made by Inverse Vulcanization. *Sulfur Chem.* **2019**, *377*, 125−151.
(14) Adekunle, K. F. A Review of Vegetable Oil-Based Polymers: Synthesis and Applications. *Open J. Polym. Chem.* **2015**, *05*, 34−40.
(15) Hoefling, A.; Lee, Y. J.; Theato, P. Sulfur-Based Polymer Composites from Vegetable Oils and Elemental Sulfur: A Sustainable Active Material for Li−S Batteries. *Macromol. Chem. Phys.* **2017**, *218*, 1600303.
(16) Valle, S. F.; Giroto, A. S.; Klaic, R.; Guimarães, G. G. F.; Ribeiro, C. Sulfur Fertilizer Based on Inverse Vulcanization Process with Soybean Oil. *Polym. Degrad. Stab.* **2019**, *162*, 102−105.
(17) Mann, M.; Kruger, J. E.; Andari, F.; McErlean, J.; Gascooke, J. R.; Smith, J. A.; Worthington, M. J. H.; McKinley, C. C. C.; Campbell, J. A.; Lewis, D. A.; Hasell, T.; Perkins, M. V.; Chalker, J. M. Sulfur Polymer Composites as Controlled-Release Fertilisers. *Org. Biomol. Chem.* **2019**, *17*, 1929−1936.
(18) Do Valle, S. F.; Giroto, A. S.; Reis, H. P. G.; Guimarães, G. G. F.; Ribeiro, C. Synergy of Phosphate-Controlled Release and Sulfur Oxidation in Novel Polysulfide Composites for Sustainable Fertilization. *J. Agric. Food Chem.* **2021**, *69*, 2392−2402.
(19) Worthington, M. J. H.; Shearer, C. J.; Esdaile, L. J.; Campbell, J. A.; Gibson, C. T.; Legg, S. K.; Yin, Y.; Lundquist, N. A.; Gascooke, J. R.; Albuquerque, I. S.; Shapter, J. G.; Andersson, G. G.; Lewis, D. A.; Bernardes, G. J. L.; Chalker, J. M. Sustainable Polysulfides for Oil Spill Remediation: Repurposing Industrial Waste for Environmental Benefit. *Adv. Sustainable Syst.* **2018**, *2*, 1800024.
(20) Lundquist, N. A.; Chalker, J. M. Confining a Spent Lead Sorbent in a Polymer Made by Inverse Vulcanization Prevents Leaching. *Sustainable Mater. Technol.* **2020**, *26*, No. e00222.
(21) Worthington, M. J. H.; Kucera, R. L.; Chalker, J. M. Green Chemistry and Polymers Made from Sulfur. *Green Chem.* **2017**, *19*, 2748−2761.
(22) *Commission Decision, 05/360/of 26 April, 2005 Establishing Ecological Criteria and the Related Assessment and Verification Requirements for the Award of the Community Eco-Label to Lubricants. Off. J. E.C., L118*, 2005.
(23) Kammann, K. P.; Phillips, A. I. Sulfurized Vegetable Oil Products as Lubricant Additives. *J. Am. Oil Chem. Soc.* **1985**, *62*, 917−923.
(24) Westcott, L. C.; Lurton, H. M. *Lubricating Composition*, 1960.
(25) Liang, D.; Zhang, Q.; Zhang, W.; Liu, L.; Liang, H.; Quirino, R. L.; Chen, J.; Liu, M.; Lu, Q.; Zhang, C. Tunable Thermo-Physical Performance of Castor Oil-Based Polyurethanes with Tailored Release of Coated Fertilizers. *J. Cleaner Prod.* **2019**, *210*, 1207−1215.
(26) Martín-Alfonso, J. E.; Valencia, C. Tribological, Rheological, and Microstructural Characterization of Oleogels Based on EVA Copolymer and Vegetables Oils for Lubricant Applications. *Tribol. Int.* **2015**, *90*, 426−434.
(27) Tonkin, S. J.; Gibson, C. T.; Campbell, J. A.; Lewis, D. A.; Karton, A.; Hasell, T.; Chalker, J. M. Chemically Induced Repair, Adhesion, and Recycling of Polymers Made by Inverse Vulcanization. *Chem. Sci.* **2020**, *11*, 5537−5546.
(28) Shankarayya Wadi, V. K.; Jena, K. K.; Khawaja, S. Z.; Yannakopoulou, K.; Fardis, M.; Mitrikas, G.; Karagianni, M.; Papavassiliou, G.; Alhassan, S. M. NMR and EPR Structural Analysis and Stability Study of Inverse Vulcanized Sulfur Copolymers. *ACS Omega* **2018**, *3*, 3330−3339.
(29) Saha, D.; Barakat, S.; Van Bramer, S. E.; Nelson, K. A.; Hensley, D. K.; Chen, J. Noncompetitive and Competitive Adsorption of Heavy Metals in Sulfur-Functionalized Ordered Mesoporous Carbon. *ACS Appl. Mater. Interfaces* **2016**, *8*, 34132−34142.
(30) Huang, L.; Shuai, Q. Facile Approach to Prepare Sulfur-Functionalized Magnetic Amide-Linked Organic Polymers for Enhanced Hg(II) Removal from Water. *ACS Sustainable Chem. Eng.* **2019**, *7*, 9957−9965.
(31) Chen, Y.; Yasin, A.; Zhang, Y.; Zan, X.; Liu, Y.; Zhang, L. Preparation and Modification of Biomass-Based Functional Rubbers for Removing Mercury(II) from Aqueous Solution. *Materials* **2020**, *13*, 632.
(32) Noirez, L.; Baroni, P.; Mendil-Jakani, H. The Missing Parameter in Rheology: Hidden Solid-like Correlations in Viscous Liquids, Polymermelts and Glass Formers. *Polym. Int.* **2009**, *58*, 962−968.
(33) Sathivel, S.; Huang, J.; Prinyawiwatkul, W. Thermal Properties and Applications of the Arrhenius Equation for Evaluating Viscosity and Oxidation Rates of Unrefined Pollock Oil. *J. Food Eng.* **2008**, *84*, 187−193.
(34) Park, C. G.; Kim, J. J.; Kim, H. K. Lipase-Mediated Synthesis of Ricinoleic Acid Vanillyl Ester and Evaluation of Antioxidant and Antibacterial Activity. *Enzyme Microb. Technol.* **2020**, *133*, 109454.
(35) Cubero-Cardoso, J.; Gómez-Villegas, P.; Santos-Martín, M.; Sayago, A.; Fernández-Recamales, Á.; Fernández de Villarán, R.; Cuadri, A. A.; Martín-Alfonso, J. E.; Borja, R.; Fermoso, F. G.; León, R.; Urbano, J. Combining Vegetable Oils and Bioactive Compounds via Inverse Vulcanization for Antioxidant and Antimicrobial Materials. *Polym. Test.* **2022**, *109*, 107546.
(36) Smith, J. A.; Mulhall, R.; Goodman, S.; Fleming, G.; Allison, H.; Raval, R.; Hasell, T. Investigating the Antibacterial Properties of Inverse Vulcanized Sulfur Polymers. *ACS Omega* **2020**, *5*, 5229−5234.
(37) Lomège, J.; Negrell, C.; Robin, J. J.; Lapinte, V.; Caillol, S. Synthesis of Alkyl Sulfur-Functionalized Oleic Acid-Based Polymethacrylates and Their Application as Viscosity Index Improvers in a Mineral Paraffinic Lube Oil. *JAOCS, J. Am. Oil Chem. Soc.* **2020**, *97*, 309−318.
(38) Araújo Junior, A. S.; Sales, W. F.; da Silva, R. B.; Costa, E. S.; Rocha Machado, Á. Lubri-Cooling and Tribological Behavior of Vegetable Oils during Milling of AISI 1045 Steel Focusing on Sustainable Manufacturing. *J. Cleaner Prod.* **2017**, *156*, 635−647.
(39) Sharma, J.; Sidhu, B. S. Investigation of Effects of Dry and near Dry Machining on AISI D2 Steel Using Vegetable Oil. *J. Cleaner Prod.* **2014**, *66*, 619−623.
(40) Murru, C.; Badía-Laíño, R.; Díaz-García, M. E. Oxidative Stability of Vegetal Oil-Based Lubricants. *ACS Sustainable Chem. Eng.* **2021**, *9*, 1459−1476.
(41) Quinchia, L. A.; Delgado, M. A.; Valencia, C.; Franco, J. M.; Gallegos, C. Viscosity Modification of Different Vegetable Oils with EVA Copolymer for Lubricant Applications. *Ind. Crops Prod.* **2010**, *32*, 607−612.

https://doi.org/10.1021/acsapm.2c00209
ACS Appl. Polym. Mater. 2022, 4, 3667−3675